X-Ray Studies on Substructures in Single Crystals of Tin. (III)

Substructures of Tin as Related to its Crystallographic Orientation

Masashige KOYAMA*

(H. Takaki Laboratory)

Received July 3, 1958

With the single crystals of tin grown in the [110] or [100] direction, the relation between the substructures and the crystallographic orientation was examined by the X-ray diffraction microscopy.

It was found in Parts I and II that the linear subboundary, which could be observed by the X-ray microscopy, developed from the reticulate subboundary of irregular shape. The same phenomenon was observed in this studies study, too. When the linear subboundary developed, its orientation difference was increased by the formation of a new corrugation along this subboundary.

I. INTRODUCTION

With the single crystals of tin grown in the [100] or [001] direction, the relation between the substructures and the crystallographic orientation was examined by the X-ray diffraction microscopy.

II. EXPERIMENTAL PROCEDURES

The purity of tin used was 99.98 % in most cases. The glass mould used, method of growing the crystal and conditions for the X-ray microscopy,** were all the same as in the previous studies (Parts I and II).

III. EXPEREMENTAL RESULTS

1. Specimens Grown in the [100] Direction

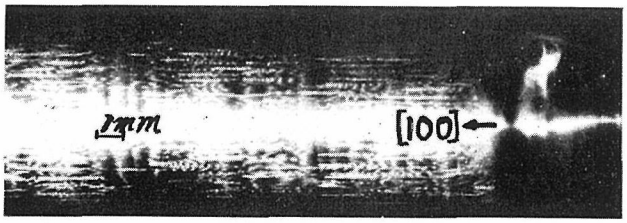

Fig. 1. Optical micrograph of the side surface (001) of the specimen (99.98 % pure tin) grown at 0.05 mm/min and 13°/cm.

* 小 山 昌 重

** Unless otherwise specified, the specimen-to-plate distance was 400 mm.

(1) Temperature gradient of 13°/cm. The examination was carried out of the single crystals grown at the speeds between 0.05 and 5mm/min. Fig. 1 shows the optical micrograph of the side surface (001) of the specimen grown at 0.05 mm/min. The streaks vertical to the direction of growth are the banding structures already reported in the previous studies. These structures are complex in shape because the purity was relatively low and the temperature gradient was small. Although corrugations are parallel to the specimen axis because of the low speed of growth, their shapes are complex.

Fig. 2. X-ray micrograph of the portion near the seed of the specimen in Fig. 1. Fe Kα, specimen face: (001), reflecting plane: (103).

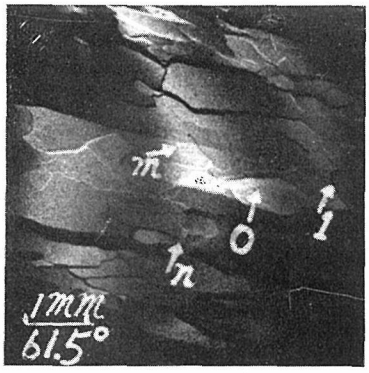

Fig. 3. X-ray micrograph of the portion fairly distant from the seed of the specimen in the Fig. 1. Fe Kα, specimen face: (001), reflecting plane: (103).

Fig. 2 shows the Berg pattern ((103) plane) of the specimen face (001) at the portion near the seed in Fig. 1, and Fig. 3 shows that of the portion fairly distant from the seed.*

The orientation diffrence of the subboundary '*m*', which developed from the seed in the direction of spcimen axis, is about 50 min of arc. The subboundary '*n*' devlops from the boundary of the substructure of irregular shape into a linear subboundary parallel to the specimen axis (its orientation difference is about 15 min of arc). As shown in Fig. 3, the orientation difference of the subboundary '*n*' is increased by the formation of a new small crystal (indicated by an arrow) which is slightly different from the neighbouring crystal in the crystallographic orientation.**

---

* When iron Kα is used, the glancing angle α becomes large because there is no other suitable reflecting plane than the (103) plane. Therefore, the width of gap or overlap of the reflected image, which indicates the orientation difference, is magnified.

** The specimen face-to-plate distance is short at the left of the photograph. Therefore, for the subboundary having the equal orientation difference, the width of gap or overlap which is observed in the reflected image must become narrower at the left. The fact that the width observed at the left is wider than that at the right would indicate that the orientation difference of this subboundary was increased with the growth of crystal.

Among the substructures observed in Figs. 2 and 3, some ones are considered to be the wavy corrugations, while the others such as indicated by r would be the ones formed after solidification.*

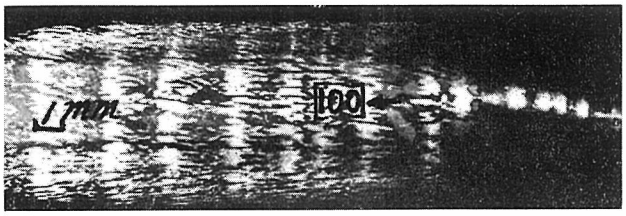

Fig. 4. Optical micrograph of the side surface (001) of the specimen (99.98 % pure tin) grown at 0.13 mm/min and 13°/cm.

Fig. 4 shows the optical micrograph of the side surface (001) of the specimen grown at 0.13 mm/min. (The direction of growth is from right to left). The banding and corrugated structures are complex in shape as compared with those shown in Fig. 1.

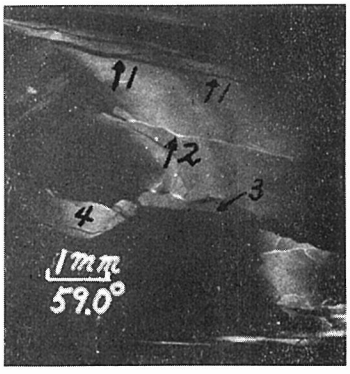

Fig. 5. X-ray micrograph of the specimen in Fig. 4.
Fe Kα, specimen face: (001), reflecting plane: (103).

Fig. 5 shows the Berg pattern ((103) plane) of the central portion of the specimen in Fig. 4. It seems that the subboundaries '1' and '2' develop from the subboundaries of irregular shape into the linear subboundaries during

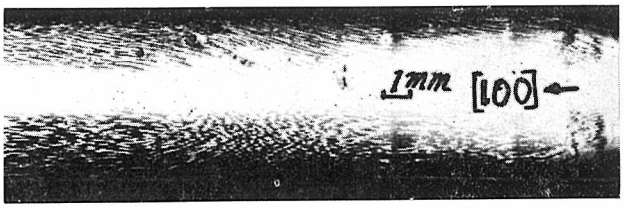

Fig. 6. Optical microgsaph of the side surface (001) of the specimen (99.98% pure tin) grown at 0.8mm/min and 13°/cm.

* As reported in Part I, a kind of fault is observed on the subboundary.

their growth. These subboundaries tend to deviate more strongly from the direction of the specimen axis toward the <110> direction with increasing speed of growth. Each of the subboundaries indicated by the marks '3' and '4', is considered to be the wavy corrugation. The substructures of smaller orientation difference are observed in the corrugation '4'.

Fig. 6 shows th opical micrograph of the side surface (001) of the specimen grown at 0.8 mm/min. (The direction of growth is from right to left). The banding structure is observed at the portion grown at a low speed (the left of the photograph). The direction of the wavy corrugation deviated more strongly toward the <110> direction than that in Fig. 4. Fig. 7 shows the Berg pattern ((103) plane) of the central portion of the specimen in Fig. 6. Besides the subboundary '1' developing from the seed, the subboundaries '2' and '3' newly formed are observed. The latter

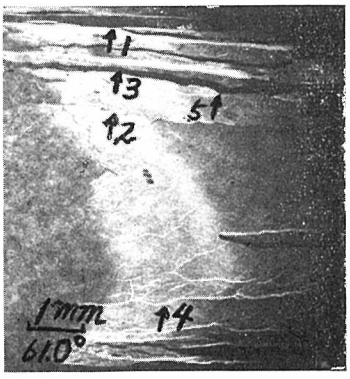

Fig. 7. X-ray micrograph of the specimen in Fig. 6. Fe Kα, specimen face : (001), reflecting plane : (103).

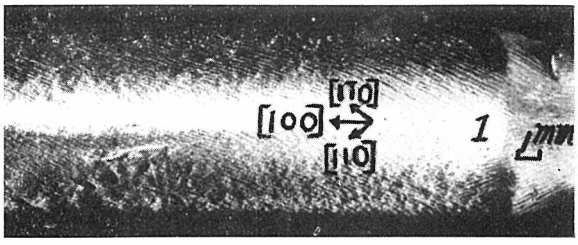

Fig. 8. Optical micrograph of the side surface (001) of the specimen (99.98 % pure tin) grown at 2.8 mm/min and 13°/cm.

two coincide with the corrugation boundary. As stated before, the orientation difference of the subboundary increases at the place (e. g. the arrow '5') where the wavy corrugation is newly formed.

Fig 8 shows the optical micrograph of the side surface (001) of the specimen grown at 2.8 mm/min. The Berg pattern ((103) plane) of the portion near the

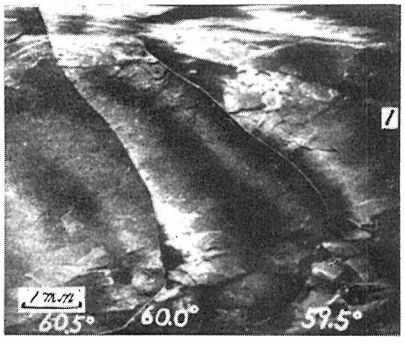

Fig. 9. X-ray micrograph of the specimen in Fig. 8. A series of reflected images taken by changing α, were jointed together. Fe Kα, specimen face : (001), reflecting plane : (103).

seed is shown in Fig. 9.* The linear subboundaries which deviate toward the <110> direction are observed in the figure. (Confer the mark '1' of Figs. 8 and 9).**

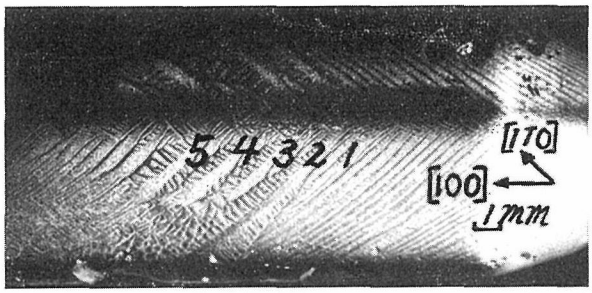

Fig. 10. Optial micrograph of the side surface (001) of the specimen (99.98% pure tin) grown at 13°/cm, in which the speed of growth was 5 mm/min in the beginning and then increased gradually up to 10 mm/min.

Fig. 10 shows the optical micrograph of the side surface (001) of the specimen grown at the speed which was 5 mm/min at first and then was increased gradually up to 10 mm/min. The dendrite structure is observed at the latter half of the specimen.

Fig. 11*** shows the Berg pattern ((332) plane) obtained by projecting X-rays in parallel to the [1$\bar{1}$0] direction of the specimen shown in Fig. 10. The boundaries

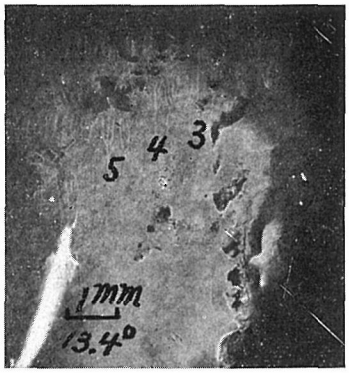

Fig. 11. X-ray micrograph of the specimen in Fig. 10. Fe Kα specimen face : (001), reflecting plane : (332).

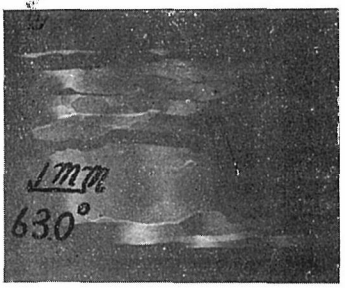

Fig. 12, X-ray micrograph of the side surface (001) of the specimen (99.98% pure tin) grown in parallel to [100] at 0.15 mm/min and 45°/cm. Fe Kα, reflecting plane : (103).

* The reflected images obtain by changing α were jointed together as done for making Fig. 10 in Part I.

** The inclination of the linear subboundary observed in Fig. 9 can not be compared with that of the corrugation boundary in Fig. 8. In the latter, the corrugations develop only in the [110] direction with the exception at the portion near the seed. This is presumably because the specimen was obliquely hung by a fine molybdeum wire in the furnace when prepared.

*** The image which is observed at the left lower part of the photograph is that of another plane.

of the dendrite arms are observed as white lines (i. e. the reflected X-rays are hard).

This is supposed to be because of the reduction of extinction by the segregation of impurities on the dendrite boundary.

(2) **Temperature gradient of 45°/cm.** In the specimen grown at 0.15 mm/min., the banding structure is seen clearer than that of the specimen in Fig. 4 and the direction of the corrugated structure is nearly parallel to that of the specimen axis. Fig. 12 shows the Berg pattern ((103) plane) of the central portion of the specimen. The linear subboundaries are more in number and deviate more strongly toward the direction of the specimen axis as compared with those in Fig. 5.

Fig. 13 shows the Berg pattern ((103) plane) of the central position of the specimen grown at 0.9 mm/min. The linear substructure increases in number with increasing speed of growth as reported in Part I.

Fig. 13. X-ray micrograph of the side surface (001) of the specimen (99.98% pure tin) grown in parallel to [100] at 0.9 mm/min and 45°/cm. Fe Kα, reflecting plane : (103).

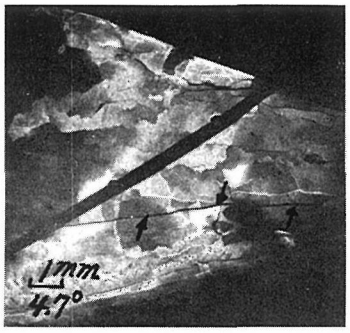

Fig. 14. X-ray micrograph of the side surface (100) of the specimen (99.98% pure tin) in parallel to [001] at 0.13 mm/min and 45°/cm. Fe Kα, reflecting plane : (301).

2. Specimen Grown in the [001] Direction

Fig. 14* shows the Berg pattern ((201) plane) of the surface (100) of the specimen grown at 45°/cm and 0.13 mm/min.

Many substructures of irregular shape are observed and some of them develop into the linear subboundaries (indicated by arrows).

In the specimen grown at 2.5 mm/min the direction of the corrugated structure is parallel to the specimen axis. Fig. 15 shows the Berg pattern ((103) plane) of the cross section (001) vertical to the axis of the specimen. The substructures which are enclosed with the subboundaries of fairly large orientation differences, are observed. Further, the subboundaries of smaller orientation difference are observed in these substructures. (The difference in the crystalographic orientation of the substructure indicated by an arrow is about 1 degree).

* This is the image of the portion near the seed of the specimen. The broad line running obliquely is a twin produced by the careless treatment.

Fig. 15. X-ray micrograph of the cross section (001) of the specimen (99.98 % pure tin) grown in parallel to [001] at 2.5 min and 45°/cm. Fe $K\alpha$, reflecting plane : (103).

IV. DISCUSSION

As reported in Parts I and II (the direction of growth was [110]), the impurity substructure (corrugation) observed microscopically is considered to have a close connection with the development of the linear substructure observed by the X-ray diffraction micorospopy.

In the microscopical examination, the corrugations deviated from the specimen axis toward the <110> direction when the specimens were grown in the [100] direction at high speeds of growth. When grown in the [001] direction, however, they were always parallel to the specimen axis. Therfore, it is interesting to investigate the relation between the linear substructure in the X-ray micrograph and the corrugated structure in the optical micrograph.

At low speeds (e. g. 0.05 mm/min), many substructuses of irregular shape were observed by the X-ray microsopy (e. g. Figs. 2 and 3). Some of them were the wavy corrugations (e. g. the substructure O in Fig. 3), while the others were formed after solidification (e. g. the subboundary *r* in Fig. 2).

The linear subboundaries which could be observed by the X-ray microscopy developed from the subboundaries of irregular shape (e. g. the subboundary '1' in Fig. 5 and the subboundary '4' in Fig. 7). In this case, the orientation difference of the subboundary increased by the development of a new corrugation along this subboundary (e. g. the subboundary 'n' in Fig. 3).

When grown in the [100] direction, the corrugations deviated more strongly toward the <110> direction with increasing speed of growth, while the linear substructures observed by the X-ray microscopy, too, deviated toward the same direction. Thus, as reported in Parts I and II, the development of the corrugations is consider to be closely connected with that of the substructure observed by the X-ray microscopy.

The same explanation made in Parts I and II could be applied in this study, the fact that the linear substructures increased in number with the increse of temperature gradient.

The boundaries of the dendrite arms were observed as white lines in the X-ray micrograph. This would be due to the fast that the quantity of impurities on the boundaries of the dendrite arms is large.

The writer wishes to express his heartful gratitude to Prof. H. Takaki for his advice and encouragement in connection with this research.

REFERENCE

(1) M. Koyama, cf. Reference (12) in Part I.